DESIGN OPTIMIZATION OF SWITCHED RELUCTANCE MOTOR FOR NOISE REDUCTION

Omid Naderi Samani – Babak Ganji*

Department of Power, Faculty of Electrical and Computer Engineering, University of Kashan, Kashan, Iran

ARTICLE INFO

***Article history*:**
Received: 5.1.2016.
Received in revised form: 15.3.2016.
Accepted: 15.3.2016.

Keywords:
Finite element analysis
Switched reluctance motor
Noise
Vibration
Simulation model
Design optimization

Abstract:

With finite element method (FEM) using ANSYS finite element (FE) package, an electromagnetic-structural simulation model is introduced for the switched reluctance motor (SRM). Since the main reason of noise and vibration in the SRM is a radial force applied to stator poles, the 2D FE transient analysis is carried out in electromagnetic modeling to predict the instantaneous radial force. Based on 3D FEM, the modal analysis is done in the developed structural model to determine mode shapes and natural frequencies. Using the developed simulation model and an evolutionary algorithm, a method is proposed for design optimization of the SRM to decrease noise. To evaluate the proposed method, the simulation results are presented for an 8/6 switched reluctance motor.

1 Introduction

Due to various advantages such as simple and rugged structure, high efficiency and good operation over a wide range of speed, special attention has been paid to the SRM in the last three decades [1]. Since the phases are excited separately, this machine can operate even under fault conditions with a reduced performance, and therefore it is a highly reliable machine. In comparison with other types of electric motor drives [2-3], SRM has the exclusive features and it can be utilized properly for different applications such as electric vehicle [4], aerospace [5], renewable energy [6-7]. However, the main drawback of this machine is its high noise which could be resolved in the future by doing more research on this topic [8].
With regard to the basic operation principles described in [9], torque in the SRM is produced by applying a DC voltage to one of the phase windings which tends to bring the rotor into a position with minimum reluctance. The different phases are excited successively and this leads to the rotor rotation. When exciting the phase, a significant attraction radial force is produced between the excited stator pole and the adjacent rotor pole. Once the excited phase has been turned off, the radial force goes off and stator vibration is suddenly released from that force. This results in the stator vibration [10].
To decrease the acoustic noise and vibration of the SRM, the various procedures have been already introduced in the literatures being divided into two major categories including the control strategies [10-12] and the machine design algorithms [13-20]. Considering different shapes for stator poles in [13-14], the best structure is suggested to minimize the noise of the SRM. To reduce the noise and vibration of the SRM, [15] introduces a special slot wedge referred to as structural stator spacers. Modeling

* Corresponding author. Tel.: 00989133250668
E-mail address: bganji@kashanu.ac.ir.

and calculating noise of the SRM, [16] shows that the 12/8 SRM produces lower noise in comparison with the 6/4 SRM. Considering various topologies for the stator structure, the most appropriate structure is introduced in [17-18] to minimize noise of the SRM. Acoustic noise and vibration in the SRM is reduced in [19] using skewed stator/ rotor poles. A multi-physics modeling of the SRM based on finite element method is introduced in [20] to simulate the acoustic radiation of the machine. In spite of the done works, we still need more research into the noise reduction of the SRM.

In the present paper, electromagnetic-structural simulation model is developed for the SRM with finite element method (FEM) using ANSYS finite element (FE) package. Carrying out the 2D FE transient analysis, the instantaneous radial force acting on the stator pole is predicted in the developed electromagnetic simulation model. In addition, modal analysis is completed in the introduced simulation model to determine mode modes and natural frequencies. The simulation model is created totally in ANSYS parametric design language (APDL) useable for different conventional types of the SRMs. The simulation model is applied to an 8/6 SRM and the simulation results including the instantaneous radial force, mode shapes and natural frequencies are given. Using a developed simulation model and an algorithm of Design of Experiments (DOE) for reducing noise and vibration, design optimization of the discussed 8/6 SRM is completed. Subsequently, the electromagnetic-structural simulation model is introduced in section 2. Applying the developed simulation model to an 8/6 typical SRM, the simulation results are presented in Section 3 and the design optimization procedure is then described. Finally, the paper is concluded in Section 4.

2 The simulation model

The developed simulation model consists of two separate parts which include electromagnetic and structural analyses. In the electromagnetic modeling, the instantaneous radial force acting on the stator pole is predicted using 2D FE transient analysis of the SRM. To predict the dynamic electromagnetic characteristics using ANSYS FE package, it is required to establish an appropriate coupling between external electric circuit and the FE model as shown in Fig. 1 for a typical 8/6 SRM. Since radial force applied to stator pole needs to be determined, the coil related to one stator pole must be considered only in the FE model. The CIRCU124 element is chosen for coupling the electric circuit to the FE model whose free node is to be connected to a node inside the coil region as observed in Fig. 1. The PLANE53 with AZ degree of freedom is selected for all regions in the FE model. Elements of coils have two extra degrees of freedom, CURR and EMF, and each slot requires a unique CURR and EMF node coupled set.

Since it is difficult to plot the geometric model of the machine each time before the analysis, the geometric model of the SRM is created as a parametric model in the FE model and the number of stator/ rotor poles, the axial length of the motor, radii of different sections, the stator and rotor pole arcs and some other geometric data are selected as geometrical parameters. A time-step analysis is required to predict dynamic electromagnetic characteristics of the SRM. In each time step, the coupling equations relating the stator and rotor at the middle of the air gap are cleared, and re-established after rotor rotation by 0.5°. The force-related boundary conditions are to be defined in the preprocessing stage using FMAGBC command and the Maxwell forces calculated on rotor elements are then to be summarized using FMAGSUM command in the post-processing stage. More details about electromagnetic modeling of the electric machines using ANSYS are accessible in [22].

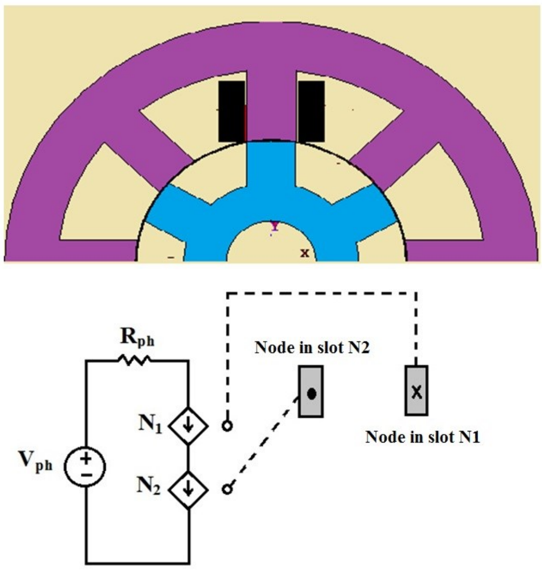

Figure 1. The FE model coupled to external circuit.

A three-dimensional structural FE analysis is carried out in the developed simulation model to study the mechanical characteristics. In order to determine the natural frequencies and mode shapes for the stator, PLANE182 and FLUID29 with Ux and Uy degrees of freedom should be utilized. When the 3D geometrical model of the stator is built up, the stage of assigned attributions is to be completed and therefore density, Young's modulus and Poisson's ratio are identified for each created volume. After meshing, modal analysis is carried out using UNSYM command and the natural frequencies and then mode shapes are determined. The frequency spectrum of the predicted radial magnetic force along with the mode shapes and the natural frequencies obtained for the stator are used to calculate vibrations. It is noted that the electromagnetic force is considered only in modeling whereas other types of forces such as aerodynamic force and those related to load coupling are not considered here.

3 Simulation results

The developed electromagnetic-structural model is applied to an 8/6 SRM, 1 kW, 1500 rpm with specifications given in Table 1 and the simulation results are presented in this section. For this motor, Young's modulus, Poisson's ratio and density are 2.07×10^{11} N/m^2, 0.3 and 7800 kg/m^3, respectively [23]. Carrying out the 2D FE transient analysis of the discussed 8/6 SRM for this operating point: phase voltage = 93 V, speed = 1500 rpm, turn-on angle = 10°, turn-off angle = 20° and single-pulse control mode, the instantaneous torque and radial force acting on the stator pole are predicted for the one phase excitation period and they are shown in Fig. 2. Using the Fourier transform, harmonics related to the predicted radial force waveform are obtained and they are illustrated in Fig. 3.

For this predicted waveform, values of the force and the corresponding frequencies are given in Table 2. The maximum force in the aligned position is 3363 N. The maximum radial force applied to the stator poles which can be seen in Fig. 4 results in stator pole displacement and vibration. For this predicted radial force, vibration distribution and the stator deformation are illustrated in Fig. 5. As it is clear from this figure, maximum pressure occurs at the corner between the stator pole and stator yoke which is 2.7×10^7 pa and the maximum displacement is 1.37×10^{-5} m.

Table 1. Motor specifications [21]

Parameter	Value
No. of phases	4
No. of stator /rotor poles	8/6
Stator outer diameter [mm]	125
Stator slot-bottom diameter [mm]	100
Rotor outer diameter [mm]	63
Rotor slot-bottom diameter [mm]	41
Air gap length [mm]	0.35
Shaft diameter [mm]	21
Stack length [mm]	90
Stator pole arc [deg.]	21
Rotor pole arc [deg.]	21
Turns per coil	124

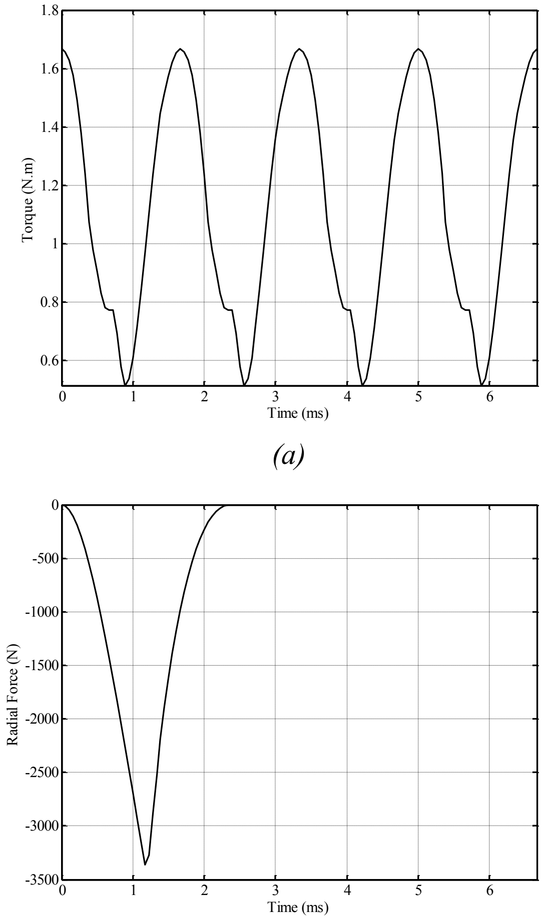

(a)

(b)

Figure 2. Predicted dynamic characteristics, (a) produced torque, (b) radial force acting on the stator pole.

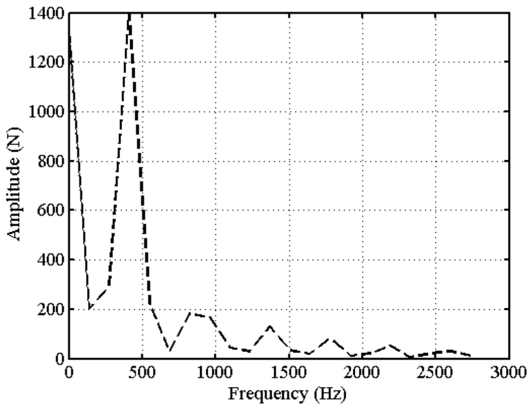

Figure 3. FFT analysis of the predicted radial force.

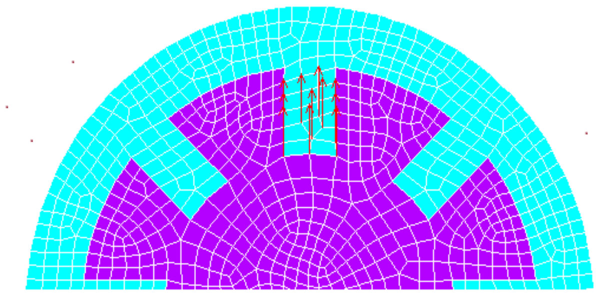

Figure 4. The load applied to the stator poles.

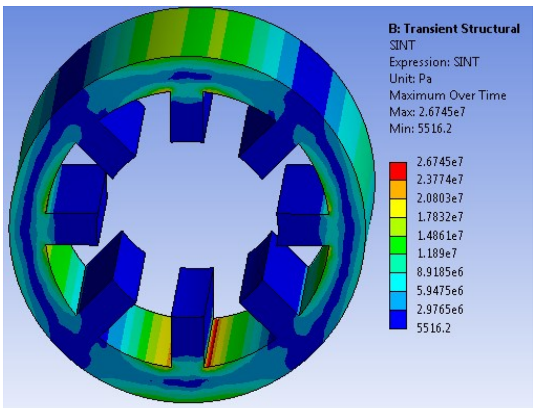

(a)

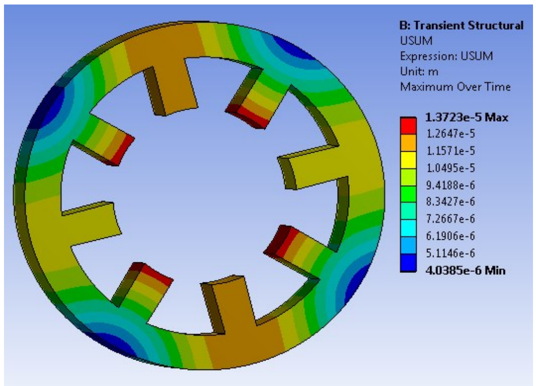

(b)

Figure 5. Results for maximum radial force, (a) vibration, (b) stator deformation.

Table 2. Calculated force for different frequencies

Harmonic	Fund.	2nd	3nd	4nd
Frequency [Hz]	237	473	710	947
Force [N]	1372	283	967	33

3.1 Design optimization procedure

In order to decrease noise of the SRM, four geometrical parameters of the stator depicted in Fig. 6 are considered in this paper and their optimal values are then obtained. In fact, these four design parameters called Tab, Fil, Tpr and Sct are considered to model the radial displacement for the stator pole, the manner of filling space between the pole and back-iron, pole tapering and stator core thickness, respectively. As Figs. 7-10 show, these selected design parameters could have significant effect on the natural frequencies. Changing these parameters for the range of Table 3, the discussed 8/6 SRM is analyzed with respect to the considered operating point using a developed simulation model and also a noise value is calculated for each design. The DOE algorithm is then used to determine the optimal design parameters for minimum noise.

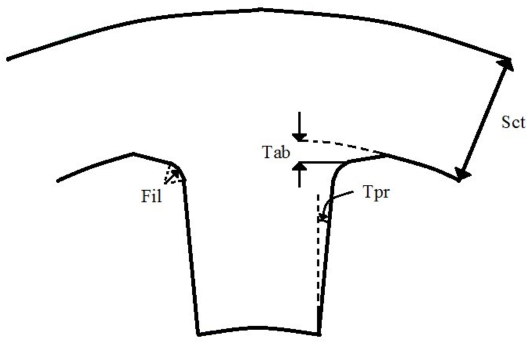

Figure 6. The selected design parameters.

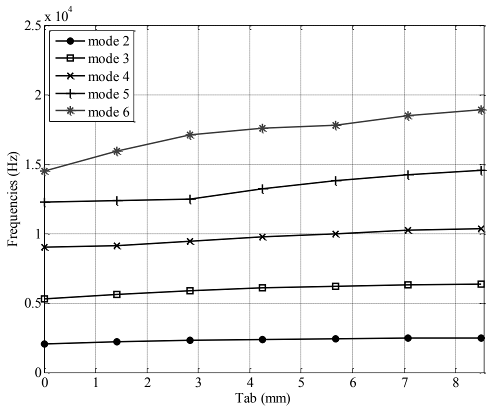

Figure 7. Influence of Tab parameter on the natural frequencies.

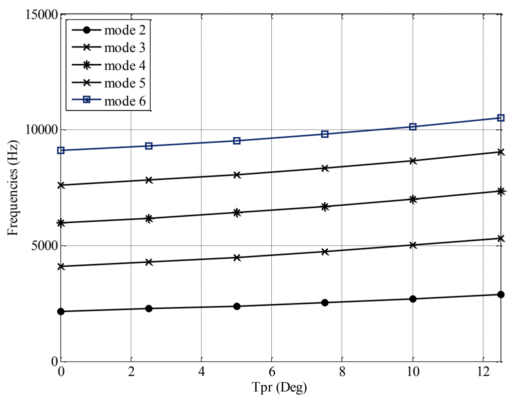

Figure 8. Influence of the Tpr parameter on the natural frequencies.

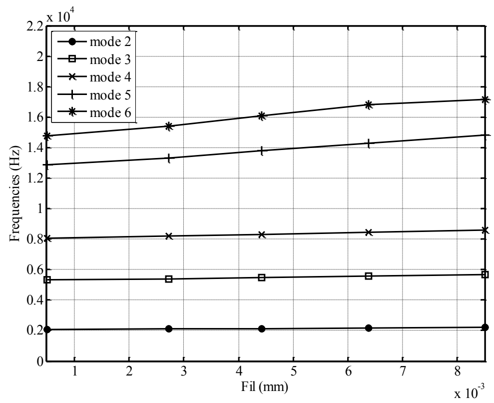

Figure 9. Influence of the Fil parameter on the natural frequencies.

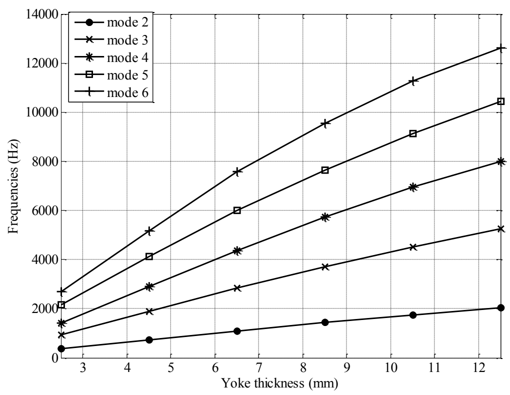

Figure 10. Influence of the Stc parameter on the natural frequencies.

The DOE is centered on factors, responses, and runs to determine whether and how a factor affects a response. The DOE is an active statistical method by which some informed changes are applied to the inputs (the selected design parameters) and then the outputs (the produced noise) are analyzed. Based on the results of output data, optimized inputs for the best outputs are obtained and utilized. There are some helpful tools, called the residual plots, used for checking whether the experiments are independent. Any special pattern on the residual plots indicates some affiliation on the experiments and it could mean the experiments are either not well-done so that their repeat orders are not appropriate or important parameters are not chosen for optimization.

Based on the design optimization procedure described above, design optimization of the available 8/6 SRM is done and the related simulation results are summarized in Table 3. In this table, the second column reveals the variations range of the selected design parameters, the third column represents the primary values of the parameters related to the available motor and the last column illustrates the obtained optimum design parameters.

Using the developed simulation model, the mode shapes and natural frequencies are obtained for both available motor and optimized motor as shown in Figs. 11 and 12. For higher natural frequencies, the possibility of resonance is lower and consequently the noise can be improved. As it is clear from these figures, the frequencies are higher for the optimized motor. The vibration plots in time domain for the two motors are compared in Fig. 13. This comparison shows that the maximum vibration is reduced to 14 m/s^2 for the optimized motor while it is 25.6 m/s^2 for the available motor. The comparison is also done for the frequency domain presented in Fig. 14 and it is seen that the proposed design optimization results in reducing the maximum vibration from 7 to 2.5 m/s^2 for the second mode which is a dominate mode. Figure 15 shows this comparison for noise signals plots in frequency domain calculated at one side of frame at 20 cm distance and it is obvious that the noise of the discussed 8/6 SRM is significantly reduced once design optimization has been done.

Table 3. Range of variations and values for the parameters

Parameter	Range of variations	Primary values	Optimum values
Tab [mm]	0 to 8.5	0	6.32
Tpr [°]	-15 to 15	0	8
Fil [mm]	0.0005 to 0.0085	0.0005	0.0055
Sct [mm]	9.4 to 18.8	12.5	14

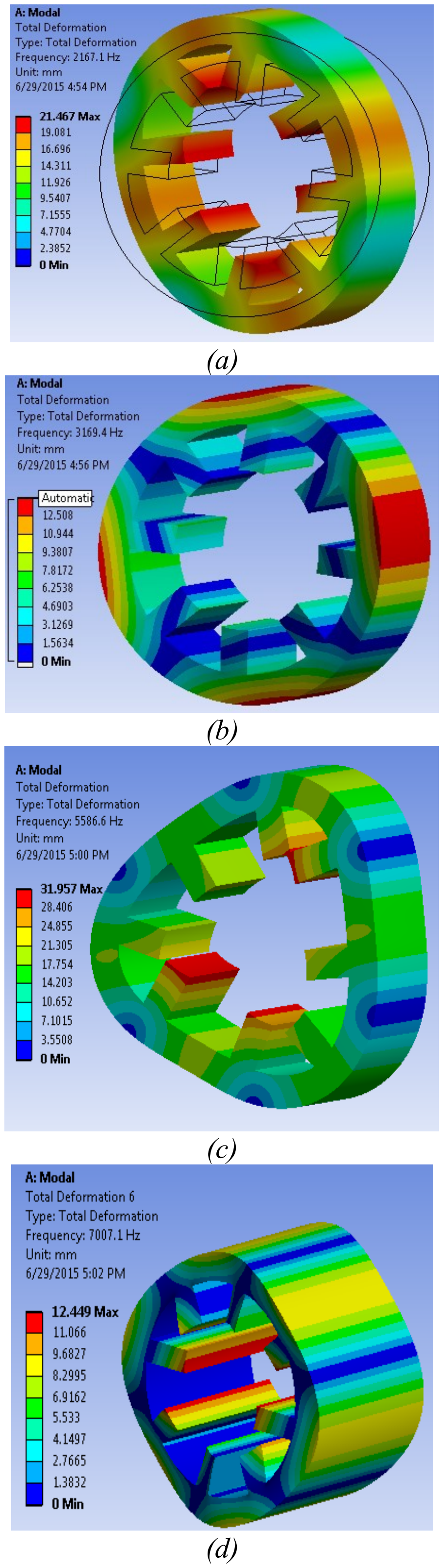

Figure 11. Stator deformation of the available motor for different modes: (a) second mode, (b) third mode, (c) fourth mode, (d) fifth mode.

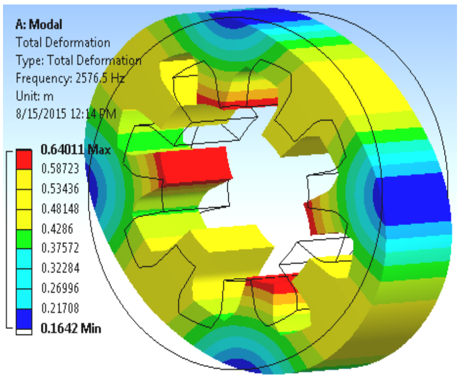

(a)

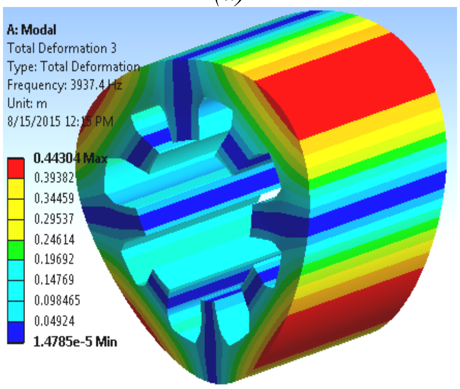

(b)

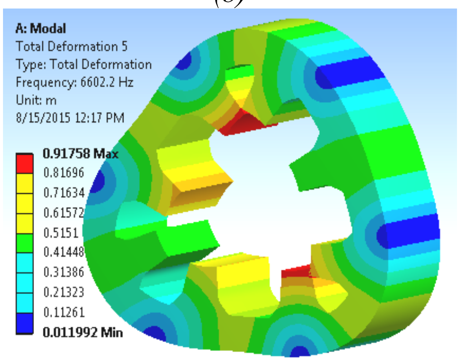

(c)

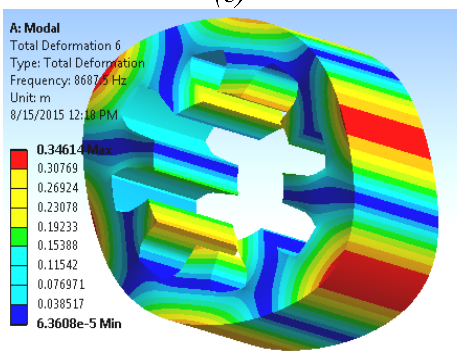

(d)

Figure 12. Stator deformation of the optimized motor for different modes: (a) second mode, (b) third mode, (c) fourth mode, (d) fifth mode.

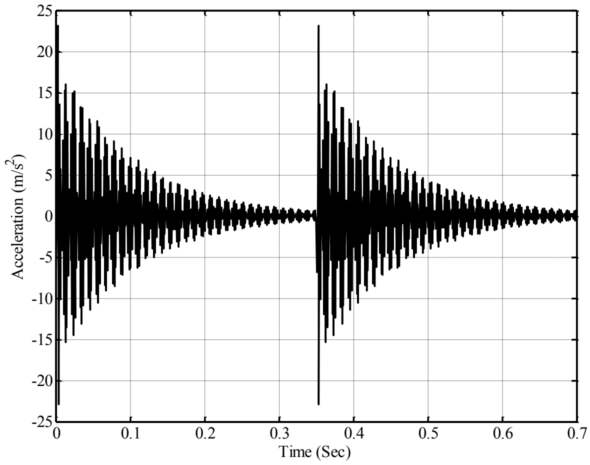

(a)

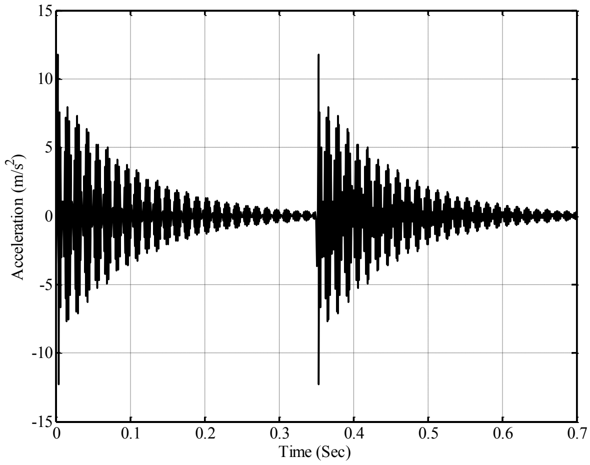

(b)

Figure 13. Vibration plots in time domain: (a) the available motor, (b) the optimized motor.

4 Summary and conclusion

An electromagnetic-structural simulation model for the switched reluctance motor was developed with ANSYS finite element package. The model is created totally in ANSYS parametric design language as a parametric model employed for different designs. In electromagnetic modeling, the instantaneous radial force acting on the stator pole is predicted precisely by carrying out 2D finite element transient analysis. The mode shapes, natural frequencies and the produced vibration due to the radial force, are calculated with 3D finite element method in the developed structural model.

Applying the introduced simulation model to an 8/6 SRM, the simulation results including instantaneous radial force, frequency modes, modes shapes and variation value were presented for the considered operating point. To reduce vibration and noise of the discussed 8/6 SRM, a design optimization procedure was described in which optimal design parameters were determined using a developed simulation model and an algorithm with Design of Experiments. The given simulation results showed a significant reduction of noise in the discussed 8/6 SRM after design optimization process.

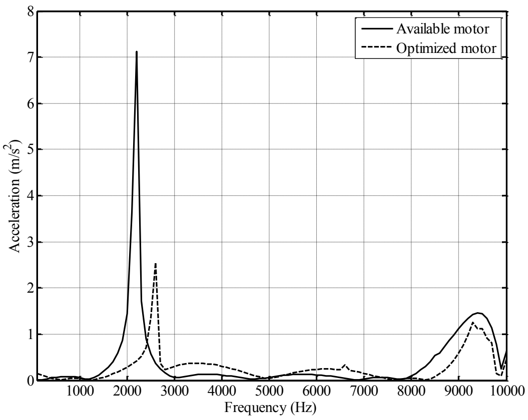

Figure 14. Vibration plots in frequency domain for the two motors.

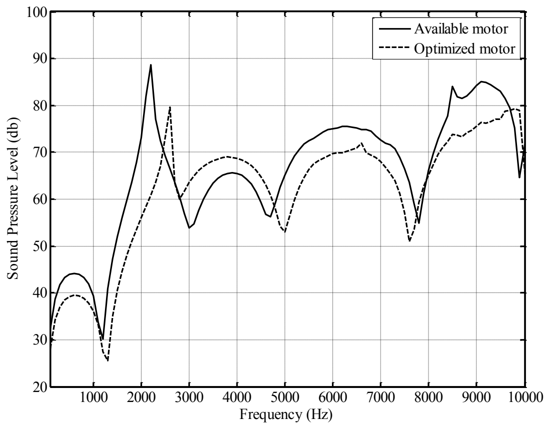

Figure 15. Noise signals plots in frequency domain for the two motors.

References

[1] Miller, T. J. E.: *Switched reluctance motor and their control*, Oxford U. K. Clarendon, 1993.

[2] Saidur, R., Mekhilef, S., Ali, M. B., Safari, A., Mohammed, H. A.: *Applications of variable speed drive (VSD) in electrical motors energy savings.* Renew. Sust. Energ. Rev., 16 (2012), 1, 543-550.

[3] Liu., Y., Wang. X., Xing. Y.,: *An improved three-level direct torque control method of brushless doubly-fed machine based on the fixed synthesizing vector,* Engineering Review, 33 (2013), 3, 203-209.

[4] Hu, K. W., Yi, P. H., Liaw, C. M.: *An EV SRM drive powered by battery/supercapacitor with G2V and V2H/V2G capabilities*, IEEE Trans. Ind. Electron., 62 (2015), 8, 4714-27.

[5] Valdivia, V., Todd, R., Bryan, F. J., Barrado, A., Lazaro, A., Forsyth, A. J.: *Behavioral modeling of a switched reluctance generator for aircraft power systems*, IEEE Trans. Ind. Electron., 61 (2014), 6, 2690-99.

[6] Choi, D., Byun, S., Cho, Y.: *A study on the maximum power control method of switched reluctance generator for wind turbine*, IEEE Trans. Magn., 50 (2014), 1, 1-4.

[7] Pan, J., Zou, Y., Cheung, N., Cao, G.: *On the voltage ripple reduction control of the linear switched reluctance generator for wave energy utilization*, IEEE Trans. Power Electron., 29 (2014), 10, 5298-5307.

[8] Miller, T. J. E.: *Optimal design of switched reluctance motors*, IEEE Trans. Ind. Electron., 49 (2002), 1, 15-27.

[9] Susnjic, L., Muzic, I.: *Switched reluctance motor simulation*, Engineering Review, 30 (2010), 1, 105-116.

[10] Cameron, D. E., Lang, J. H., Umans, S. D.: *The origin and reduction of acoustic noise in doubly salient variable-reluctance*, IEEE Trans. Ind. Appl., 28 (1992), 6, 1250-55.

[11] Wu, C. Y., Pollock, C.: *Analysis and reduction of vibration and acoustic noise in the switched reluctance drive*, IEEE Trans. Ind. Appl., 31 (1995), 1, 91-98.

[12] Takiguchi, M., Sugimoto, H., Kurihara, N., Chiba, A.: *Acoustic noise and vibration reduction of SRM by elimination of third harmonic component in sum of radial forces*, IEEE Trans. Energy Convers., 30 (2015), 3, 883-91.

[13] Hong, J. P., Ha, K. H., Lee, J.: *Stator pole and yoke design for vibration reduction of switched reluctance motor*, IEEE Trans. Magn., 38 (2002), 2, 929-932.

[14] Kotegawa, T., Miki I.: *Stator structure for reducing noise in switched reluctance motor*,

European Conference on Power Electronics and Applications, 2013, 1-9.

[15] Rasmussen, P. O., Andreasen, J. H., Pijanowski, J. M.: *Structural stator spacers- a solution for noise reduction of switched reluctance motors*, IEEE Trans. Ind. Appl., 40 (2004), 2, 574-81.

[16] Li, J., Song, X., Cho, Y.: *Comparison of 12/8 and 6/4 switched reluctance motor: noise and vibration aspects*, IEEE Trans. Magn., 44 (2008), 11, 4131-34.

[17] Pillay, P., Cai, W.: *An investigation into vibration in switched reluctance motors*, IEEE Trans. Ind. Appl., 35 (1999), 3, 589-96.

[18] Li, J., Cho, Y.: *Investigation into reduction of vibration and acoustic noise in switched reluctance motors in radial force excitation and frame transfer function aspects*, IEEE Trans. Magn., 45 (2009), 10, 4664-67.

[19] Yang, H., Lim, Y., Kim, H.: *Acoustic noise/vibration reduction of a single-phase SRM using skewed stator and rotor*, IEEE Trans. Ind. Electron., 60 (2013), 10, 4292-4300.

[20] Santos, F. L. M., Anthonis, J., Naclerio, F., Gyselinck, J. J. C., Auweraer, H., Goes, L. C. S.: *Multiphysics NVH modeling: simulation of a switched reluctance motor for an electric vehicle*, IEEE Trans. Ind. Electron., 61 (2014), 1, 469-76.

[21] Ganji, B., Faiz, J., Kasper, K. A., Carstensen, C. E., DeDoncker, R. W.: *Core loss model based on finite element method for switched reluctance machines*, IET Elec. Power Appl., 4 (2010), 7, 569-77.

[22] Faiz, J., Ganji, B., DeDoncker R.W., Fiedler J.: *Electromagnetic modeling of switched reluctance motor using FEM*, 32nd Annual Conference of the IEEE Industrial Electronics Society, 2006, 1557-1562.

[23] Fiedler, J. O., Kasper, K. A., DeDoncker, R. W.: *Calculation of the acoustic noise spectrum of SRM using modal superposition*, IEEE Trans. Ind. Electron., 57 (2010), 9, 2939-45.